# Model Assisted Probability of Detection for NASA Space Missions

Elizabeth GREGORY [1], Peter JUAREZ [1], William SCHNECK [1], Geoffrey Bomarito[1]
[1] NASA Langley Research Center, Hampton, USA

Contact e-mail: [Elizabeth.D.Gregory@nasa.gov]

**Abstract.** Model assisted probability of detection (MAPOD) uses data from simulations to improve a traditional probability of detection (POD) study. This could include extending the parameter space to reduce uncertainty or substituting experimental data with simulated data to reduce the time and cost of a POD study. In the past MAPOD was difficult due to limited computational resources, but recent innovations in simulation tools and high-performance computing have made this type of high-degree-of-freedom modeling possible, and complex structures have made it necessary.

This presentation will summarize the work done by the computational nondestructive evaluation (CNDE) specialists within the Nondestructive Evaluation Sciences branch at NASA Langley Research Center (LaRC) to complete a MAPOD study for phased array ultrasound testing (PAUT) of a friction stir welding (FSW) method to be used on Space Launch System (SLS) structures. The three critical needs for a MAPOD study are a validated and verified model of the inspection technique for the structure being inspected, some experimental POD data, and an uncertainty model for both the model and the experimental data. PAUT was simulated using Extende CIVA's UT module. The model was validated using laboratory inspection data from NASA Marshall Space Flight Center (MSFC) for a Hit/Miss POD for FSW in 2219-T87 aluminum panels representative of those used in the SLS.

This model was then used to simulate flaw sizes that were originally omitted from the original POD study. The results of this new MAPOD study will be presented along with a discussion of the methods and processes used to analyze the original data, selected simulation parameters, and development of the uncertainty model used for the statistical analysis. The goal of this effort is not just to improve the POD study but to demonstrate the value of MAPOD and provide a roadmap for application of MAPOD on future projects.

## 1 Introduction

NASA's long-term goals include fabrication and assembly of structures in orbit. This is an ambitious goal and will require the inspection and certification of structures for the extreme environment of space. The already time consuming and costly activity of inspection will become even more complex and costly in this new workflow. The field of nondestructive evaluation (NDE) , which includes nondestructive inspections and testing (NDI & NDT), must leverage cutting edge computing resources and data analysis techniques to transform these previously manual processes into one where inspectors employ automation and simulation to reduce time and cost. This is the role of computational nondestructive evaluation (CNDE). CNDE aims it reduce time and cost by eliminating unnecessary physical testing and improve confidence in results with supporting simulated data.

This work illustrates the process by which a probability of detection study can be made less costly and time consuming by combining simulation and modeling data with experimental data to reach the same results.

## 1.1 Probability of Detection

For the certification of an inspection process for a specific structure, a probability of detection (POD) study must be completed to determine the limits of the inspection process for that structure [1]. A traditional POD study is a strictly defined process [2]. Typically, a POD study consists of many test specimens that are representative of the structure that will be inspected. These test articles must include representative flaws of a range of sizes and may also include other variability, such as ranges of possible flaw orientations. Every test specimen is inspected with the selected modality, and the indication is recorded. This indication may be a measured signal response or a binary hit/miss record.

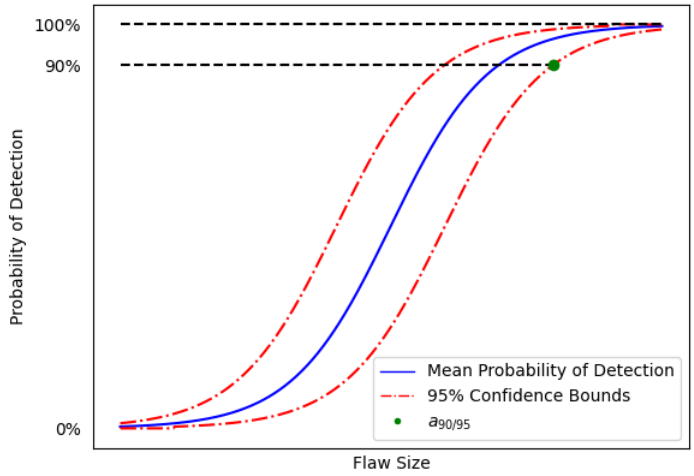



**Figure 1** Demonstrative POD curve with $a_{90/95}$ and 95% confidence bounds.

Figure 1 shows an example of a hit/miss POD curve plotting the probability that a flaw is detected as a function of the flaw size. It is created from the presence (hit) or absence (miss) of a flaw indication in the inspection data. Figure 1 show the mean probability of detecting a flaw of a specific size (the solid blue line) and the 95% confidence bounds of that probability (the dashed red line). The metric that is most often reported from this type of plot is $a_{90/95}$ which is the flaw size that has a 90% probability of being detected with 95% confidence [3, 4]. The inspection for this structure is assumed to be able to detect flaws larger than this and not reliably detect flaws smaller than this.

## 1.2 Model Assisted Probability of Detection

As previously stated, POD requires many test specimens and many inspections. Although 60 specimens may be sufficient for some applications, confidence and quality is very often improved by including more specimens. As the number of specimens increases, it is obvious that a POD study can quickly become expensive, and the duration of the study could become prohibitively long. In order to reduce this burden, NDE professionals proposed Model Assisted Probability of Detection (MAPOD) [5]. MAPOD is the process by which experimental data is augmented by simulating data using a validated model of the inspection process and specimens [6]. Simulation can be used to complete the data set needed to create a POD curve, or to add data to an existing POD curve to enhance the accuracy. It is not recommended that modeling replace all experimentation for the POD process. At a minimum, experimentation is necessary for validation of the model.

### 1.3 Friction Stir Welding

In this work the value of MAPOD was demonstrated using data from friction stir welded panels. Friction stir welding (FSW) is the process by which two metallic pieces are joined by generating sufficient heat with a rotating tool that softens the material and intermixes it, thereby creating a unified volume as the rotating tool moves along the seam.

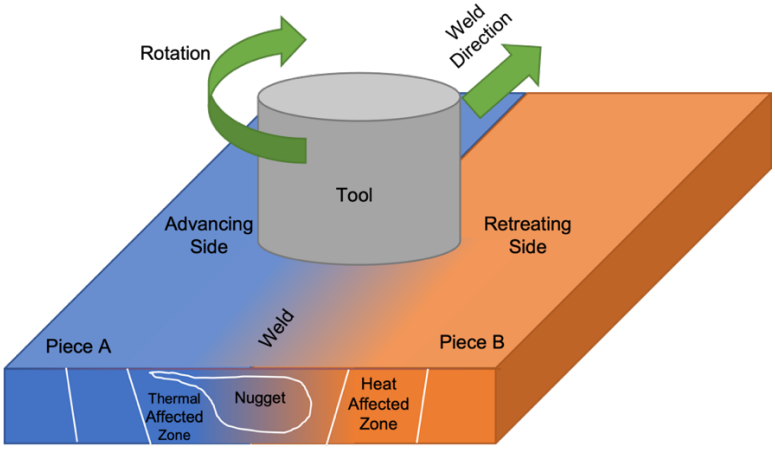



**Figure 2** Friction stir welding process and internal structure.

Figure 2 is an illustration demonstrating how the tool interacts with the original two pieces (labelled A and B). It also shows the internal structure that is left in the wake of the welding process. There are three unique zones created by the welding process, namely the Heat Affected Zone, the Thermal Mechanical Affected Zone, and the Nugget. Each may have different grain structures and material properties, the most pertinent of which for this work is transverse wave speed.



**Figure 3** SLS Launch Vehicle Stage Adapter test article includes friction stir welds that must be inspected with a certified inspection process.

## 2 Original Probability of Detection Study

As part of studying friction stir welding for upcoming space structure applications, such as the SLS Launch Vehicle stage adaptor shown Figure 3, Marshall Space Flight Center conducted a POD study on artificial cracks in FSW panels.

The experimental data consisted of 88 Electrical Discharge Machined (EDM) notches to emulate cracks spread over five panels. Each panel was the result of friction stir welding two AL2219-T87 aluminum pieces together along their longest sides. Each of the

EDM notches were placed in the weld at different places along the length of the panel and their location along the length was recorded as being in one of 17 zones defined sequentially along the length. Each zone was assumed to be identical; therefore, the position along the length is not a defining characteristic.

Each EDM notch was located at the top and bottom surfaces, referred to as the "crown" or "root" of the weld, respectively. Across the width of the weld, each EDM notch was located at one of three locations: the advancing side (meaning that edge of the rotating tool was moving in the same direction as the weld path), the retreating side (meaning that edge of the rotating tool was moving in the opposite direction as the weld path), and the center of the weld. Therefore, each EDM notch was located in three-dimensions by defining its zone, crown or root; and advancing side (AS), retreating side (RS), or center (CT). The other characteristics of the notches were length, depth, and skew. Skew angle is the angle with respect to the weld path, 0° meaning the length of the crack was parallel to the weld path and with 90° being perpendicular. Each EDM notch had a skew of 0°, 45° or 90°.

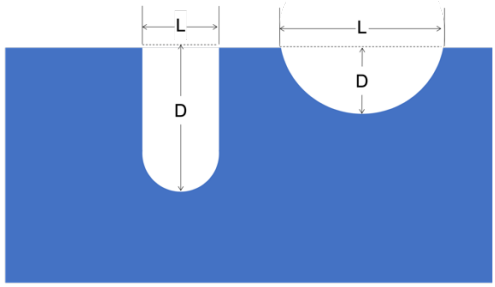



**Figure 4** Assumed EDM notch area used to calculate area for the POD study base on notch length (L) and depth (D).

The POD was finding probability of detecting a flaw of a certain area. Figure 4 shows the assumed areas for the EDM notches based on the length and depth measured. These areas are idealized. Shapes of the notches were assumed to be different depending on the ratio of length to depth. The area use for the POD study was calculated as:

$$A_C = \begin{cases} \pi\frac{L^2}{8} + \left(D - \frac{L}{2}\right)\cdot L, & \frac{L}{2} \le D \\ \frac{r_c^2}{2}(\theta - \sin\theta), & \frac{L}{2} > D \end{cases}$$

**Equation 1**

where the radius of curvature, $r_c$, and the angle of the arc, θ, are:

$$r_c = \frac{D}{2} + \frac{L^2}{2D} \qquad \theta = 2\sin^{-1}\left(\frac{L}{2r_c}\right) + \frac{L^2}{2D}$$

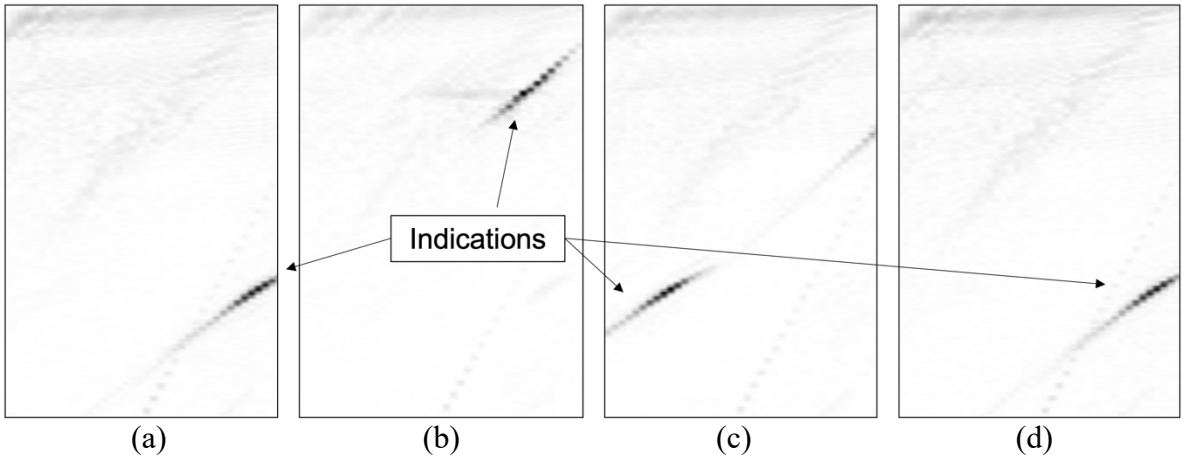



**Figure 5** Example of experimental phased array UT inspection E-Scans for EDM notches (a) located on the center of the weld at the root, (b) located on the advancing side at the crown, (c) located on the retreating side at the root, and (d) located on the advancing side root.

The panels were inspected with UT phased array (PAUT) and then based on an established threshold an indication corresponding to a crack was determined to be a 'Hit' if its peak indication was above the threshold and a 'Miss' if it was below the threshold. Each panel was scanned at three orientations (0°, 90°, & 270° with respect to the weld path) for two beam refracted angles (45° & 60°) for a total of six unique scan configurations. Figure 5 shows the PAUT responses in E-scans for four cracks at four different locations along the weld and at both the root and the crown.

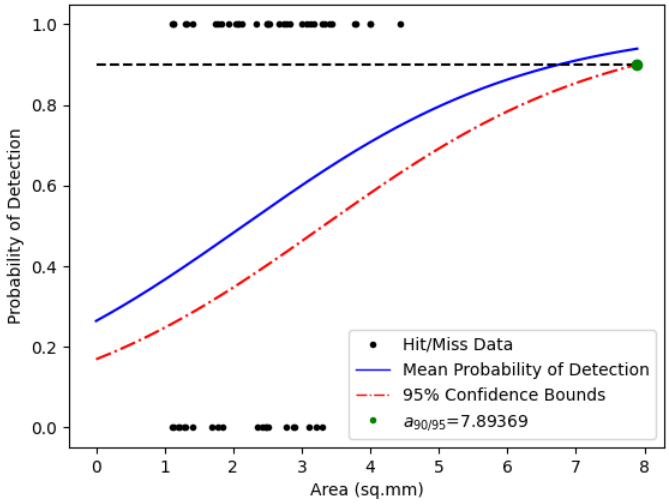



**Figure 6** POD Curve based on experimental data

Of the 88 EDM notches placed, 60 met the criteria to be considered a 'Hit' and 28 were considered 'Misses'. Figure 6 show the resulting POD curve and the calculated $a_{90/95}$ was found be 7.894 $mm^2$. One serious issue with this study was the POD curve did not cross the 90% probability of detection level, within the range of flaw sizes considered in the study. This issue provides an opportunity for simulation to supplement limitation present in the prior experimental work.

## 3 Modeling Phased Array UT in Friction Stir Welds

Early in the process CIVA [7] was selected to model the phased array UT inspection of the friction stir welds. CIVA is a semi-analytical/numerical NDE simulation code.

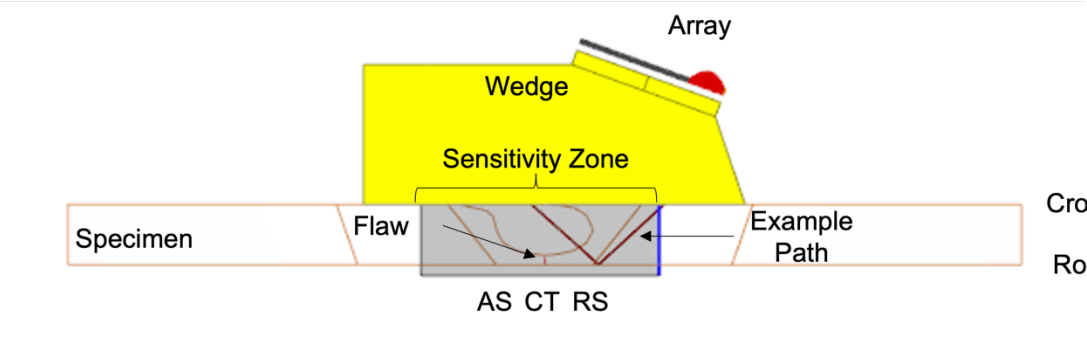



**Figure 7** CIVA Model of phased array UT inspection on a friction stir weld.

Figure 7 Shows the CIVA model that was created with the probe, internal structure and a single flaw, located at the center of the weld (CT) on the root surface. The model was of a small length of weld. Probe and signal parameters were provided with the experimental data so those were used in the model. Modeling FSW is somewhat complicated due to the internal weld structure. CIVA allows defining grain structure for metallic structures. The FSW process created zones of complex grain orientations which were modelled as polycrystalline materials. The material properties were estimated from literature reviews and analysis of the inspection data.

Just as the panels were scanned with six different configurations of orientation and beam refracted angle, initially it was assumed only six simulation configurations would be necessary. However, after initial development it was clear that separate simulations would be necessary for Root and Crown defects as the near and far field effects for each were different.

### 3.1 Model Validation and Verification

Validation and Verification of any model is critical to establishing trust in the results of that model. It is not merely sufficient to say that the results "look" right or that the inputs into the model be correct. Verification is answering the question "Is the modeling solving the problem correctly?" In this case CIVA has demonstrated repeatedly that their algorithms are correctly executing the underlying physics of multiple NDE modalities, including PAUT. Validation poses and more complex question: "Does the model reflect reality?" For the application of MAPOD this is the crux of the problem. There is no perfect model of reality and if there was it would most likely be extremely expensive and compute intensive. Engineers must determine what aspects of reality are most pertinent to the problem they are trying to solve and focus on modeling those aspects.

For this model the validation method selected was a goodness-of-fit method for a small group of experimental datasets. "Goodness-of-Fit" is being used in this context as a descriptor of the degree of similarity of the model and the experimental data. The metric used to compare the experimental data with the simulated data was the relative indication of signal location and shape. This was done by recording the max amplitude for each element. This creates a profile for each scan and each simulation. By only recording the maximum amplitude value and not where (when) it occurred ignores the time of flight which is primarily a function of material properties. The goal was to compare the location of the flaws and the shape of the indication. The amplitudes were normalized. The peak usually occurs across different elements. The location error is described by the offset between the peaks and the shape error is described by to be sum squared error after the peaks are aligned.

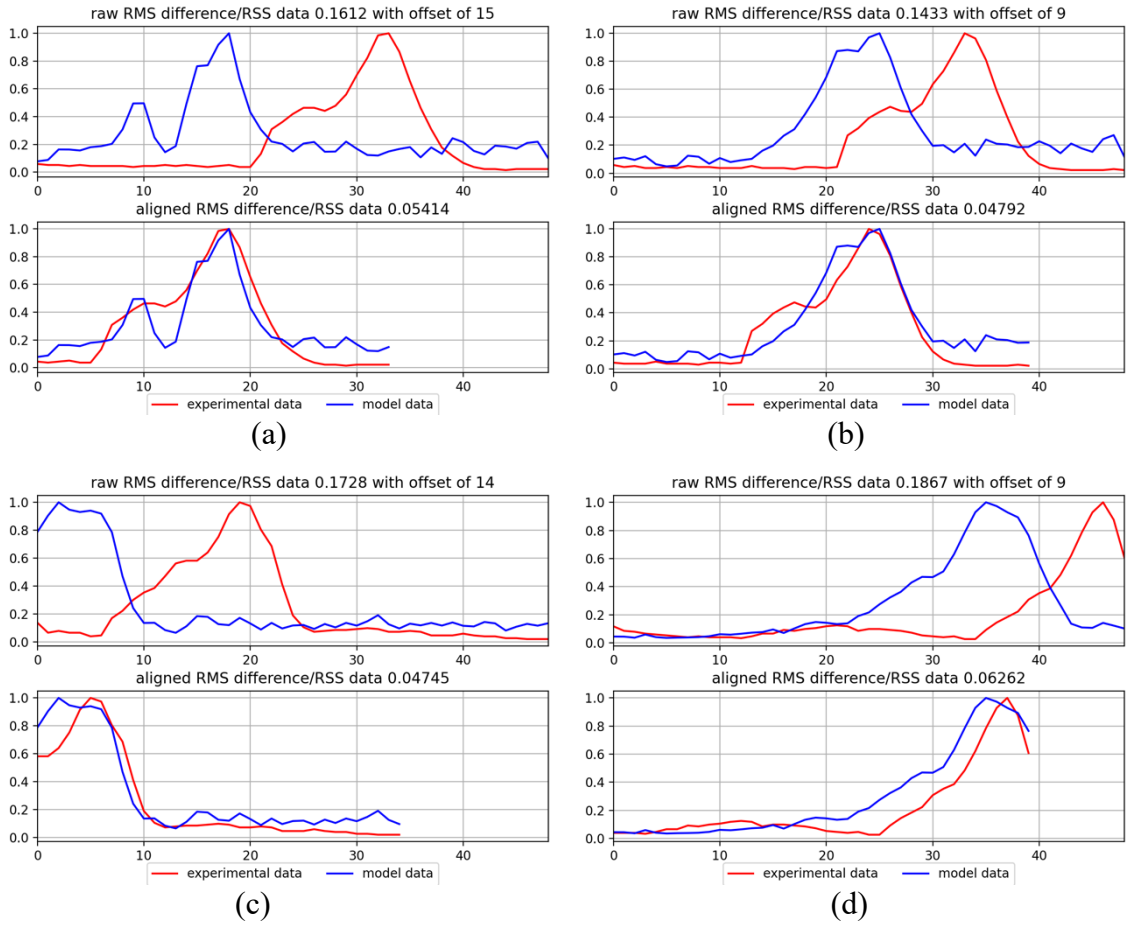



**Figure 8** Validation plot comparing experimental vs simulation PAUT of friction stir welds with EDM notches located at the Root. (a) Simulation with a 90° orientation of an EDM notch located on the center line. (b) Simulation with a 270° orientation of an EDM notch located on the center line. (c) Simulation with a 90° orientation of an EDM notch located on the retreating side. (d) Simulation with a 270° orientation of an EDM notch located on the retreating side.

Figure 8 shows four plots of two inspection configurations of two EDM notches. Their offsets were consistent across simulation configurations (i.e. 14 for 90° orientation and 9 for 270° orientation). The simulations for the root EDM notches (shown here) had shape errors of less than 0.9 for the validation set of EDM notches. Each of the experimental hit/miss calls made for the notches in the validation set were the same as the calls made with the simulation data, meaning if it was a 'hit' in the laboratory it was also a 'hit' according to the simulation. These metrics were considered sufficient to validate the models for the root notches.

## 4 Results & Conclusions

This work utilized a pre-existing POD study of limited size for PAUT inspection of EDM notches in friction stir welds. A subset of eight scans from the experimental data made up a validation set that was used to validate a CIVA model of the inspection. After validation a larger set of 22 EDM notches (that did not include the validation scans) were simulated. The simulation scans were analyzed using the same criteria for determining a 'hit' or miss' as that used in the POD study. Each of the 22 notches' call of hit or miss were the same for the simulation as it was in the experiment. The POD study conclusions would not have changed by using up to 25% simulated data.

In the future, a small set of initial data could be gathered experimentally to validate a model and then the validated model could be used to create data for some of the POD study, reducing the time necessary to manufacture and inspect the specimens as well as the cost of material. This study only completed validation of three of the six necessary inspection configurations: orientation of 90° with beam refracted angle of 45° and orientation of 270° with beam refracted angle of 45° and 60°. It is possible that an even larger amount of the data could be simulated while finding the same results.

The original POD study was limited by the number EDM notches that could be made and inspected. Reviewing Figure 6, it shows that the calculated $a_{90/95}$ is far outside the population of areas of tested notches. It would be possible to test a few larger EDM notches and use that data to further validate the model and then generate sufficient data for a population of notches with larger areas. This work demonstrates the value and feasibility for model assisted POD for PAUT of friction stir welds.

## 5 Acknowledgements

The authors would like to acknowledge the guidance and insight provided by John Aldrin of Computational Tools. James Walker, Jason Eldridge and Samuel Russall of the EM21 group at NASA Marshall Space Flight Center provided the original phased array UT inspection data and corresponding POD study, as well as significant information about friction stir welding.

This work was funded by the Langley Research Center ACT2 program, the Transformation Tools and Technology (TTT) program, and an internal IRAD grant form Langley Research Center.

## 6 References

1. NASA, "Nondestructive Evaluation Requirements for Fracture-Critical Metallic Components," Standard NASA-STD-5009B, May 2019.
2. US Department of Defense, "Nondestructive Evaluation System Reliability Assessment Mil-Hdbk-1823a," United States Depeartment of Defense, United States, MIL-HDBK-1823A, Apr. 2009.
3. D. Olin and Q. Meeker, "Applications of Statistical Methods to Nondestructive Evaluation," *American Statistical Association and the American Society for Quality Control TECHNOMETRICS,* vol. 38, no. 2, p. 18, 1996.
4. E. A. Lindgren, D. S. Forsyth, J. C. Aldrin, and Spencer, "Probability of Detection," in *Nondestructive Evaluation of Materials*, A. Ahmad and L. J. Bond, Eds. ASM International, 2018, pp. 8–22.
5. R. M. Meyer, S. L. Crawford, J. P. Lareau, and M. T. Anderson, "Review of Literature for Model Assisted Probability of Detection," Pacific Northwest National Lab. (PNNL), Richland, WA (United States), PNNL-23714, Sep. 2014.
6. Tuomas Koskinen and Iikka Vikunin, "Hit/Miss POD with Model Assisted and Emulated Flaws," presented at the The 12th ECNDT, Gothenburg, SE, 2018.
7. "EXTENDE, Experts in Non Destructive Testing Simulation with CIVA Software." https://www.extende.com/.